Enhancing Pharmaceutical Crystallization in a Flow Crystallizer With Ultrasound: Anti-Solvent Crystallization

Hussain M.N.[1], Jordens J.[1], John J.J.[1], Braeken L.[2], Van Gerven T.[1]*

[1]Department of Chemical Engineering, KU Leuven, 3001 Leuven, Belgium

[2]Faculty of Engineering Technology, KU Leuven, Agoralaan Building B Box 8, 3590 Diepenbeek, Belgium

*Corresponding author: tom.vangerven@kuleuven.be

Highlights

- Anti-solvent crystallization of ASA-Aspirin was studied in silent and sonicated flow conditions
- Ultrasound significantly accelerated nucleation and enabled crystallization even at low supersaturation levels
- Continuous crystallization was achieved at as low as 48 wt. % of anti-solvent and supersaturation of 1.02
- Using lower power ultrasound was more effective in achieving continuous crystallization without loss in yield

Enhancing Pharmaceutical Crystallization in a Flow Crystallizer With Ultrasound: Anti-Solvent Crystallization

Hussain M.N.[1], Jordens J.[1], John J.J.[1], Braeken L.[2], Van Gerven T.[1]*

[1]Department of Chemical Engineering, KU Leuven, 3001 Leuven, Belgium

[2]Faculty of Engineering Technology, KU Leuven, Agoralaan Building B Box 8, 3590 Diepenbeek, Belgium

*Corresponding author: tom.vangerven@kuleuven.be

Abstract

Continuous crystallization is a fast growing application domain in the pharmaceutical industry. Application of ultrasound has been proven to have positive effects like reduction in induction time and Metastable Zone Width (MSZW) in both batch and flow systems. Further understanding of flow-based sonocrystallization is required to achieve industrial level scale up. This work investigates the sonocrystallization of pharmaceutical compounds in a tubular flow crystallizer. Acetyl Salicylic Acid (ASA-Aspirin) is used as a model compound with ethanol and water as solvent and anti-solvent, respectively. Experiments were conducted in silent and sonicated conditions to study the MSZW. Ultrasound made it possible to achieve crystallization within the crystallizer which was not possible in silent conditions, under the tested conditions. Continuous crystallization was achieved at as low as 48 wt. % of anti-solvent and supersaturation of 1.02. In some experiments, temperature rise with ultrasound caused the crystals to re-dissolve within the channels. Better crystallization - no re-dissolution - was achieved by using low ultrasonic power without any loss in the yield. Particle sizes of product crystals were in the range of 4 – 46 µm. In conclusion, ultrasound was highly effective in enabling anti-solvent crystallization of a pharmaceutical compound in a tubular flow crystallizer.

Introduction

In the pharmaceutical industry 90% of the products are crystalline organic compounds that need refining via recrystallization processes [1] [2]. Traditional industrial recrystallization procedures are predominantly conducted via batch methods. The problems associated with batches, such as batch-to-batch variability, larger equipment, higher costs etc., are well known [3]. Crystallization is a stochastic process which is influenced by many factors, for e.g. presence of impurities, additives, mixing level, heat transfer, materials etc. [4]. The stochasticity of crystallization manifests itself in the outcome as variability in induction time, particle sizes etc. This is attributed to the intrinsic stochastic or unpredictable nature of nuclei formation which has many pathways but mainly homogeneous, heterogeneous and secondary nucleation. These factors make crystallization difficult to rationalize and control and also pose problems for scale up [5]. Crystallization in flow, in essence, is a process intensification technique that provides miniaturization by reducing the control volume compared to batch reactors. This allows homogeneous application of process parameters (e.g. supersaturation, temperature) that are required to achieve desired properties such as particle size, shape, polymorph selectivity etc. Tubular crystallizers provide better reproducibility and efficiency due to narrow residence time distribution and reduction in secondary nucleation effects but also have the problem of fouling and more complicated equipment [3] [6]. However, tubular crystallizers provide a better scope for scale up than mixed suspension and mixed product removal (MSMPR) type continuous crystallizers [6]. They provide desired benefits like faster supersaturation achievement especially in anti-solvent crystallization by enabling rapid mixing, stable conditions at steady state of operation, narrower crystal size distribution as a result of better supersaturation homogeneity etc.

Among the solvent mediated crystallization techniques, the most prevalent ones are cooling, reactive and anti-solvent crystallization types. Anti-solvent crystallization basically involves mixing of two miscible fluids: a solution of the Active Pharmaceutical Ingredient (API) and the anti-solvent. Mixing enhances local supersaturation homogeneity (spatial), thus crystallizing the API [7]. Anti-solvent crystallization can be conducted at constant temperature, which is an incentive for flow crystallization because it reduces process complexity. The effectiveness of a continuous flow, anti-solvent crystallization system is dependent on the mixing, therefore, some techniques must be applied to have a well-mixed system. This is of specific importance in tubular crystallizers since conventional stirring methods like stirrers are not easy to integrate. Static mixers are an option but they require higher velocities for effective mixing and are prone to clogging [1]. Ultrasound is another technique to improve mixing in tubular crystallizer systems for anti-solvent crystallization. Ultrasound basically consists of pressure waves being generated in a system above a certain frequency (20 kHz – 0.8 MHz). These pressure waves improve mixing [8] [9]. An important effect of ultrasound, under certain process conditions, is cavitation. During the negative cycle of the pressure wave, cavitation voids are formed in fluid systems which have internal high temperatures and pressures. When the cavitation bubbles implode, they create jets of fluid and shock waves that enhance local mixing [8]. At lower frequencies, transient cavitation, which yields stronger implosions, dominates and improves mixing much better [10]. Cavitation could also have local cooling effects due to bubble expansion and can sometimes act as foreign particles causing heterogeneous nucleation [11]. Although the exact effect of ultrasound may be subjective and difficult to determine, there is consensus that cavitation affects crystallization [12] [13]. In many cases ultrasound has proven to reduce the induction time and reduce the Metastable Zone Width (MSZW) [8] [9] [12] [13] [14]. In addition, ultrasound is also known to reduce clogging which makes it suitable for tubular crystallizers. Ultrasound is becoming more popular in the pharmaceutical industry with companies like *GlaxoSmithKline* and *Abbott* using ultrasound for producing medicines like Paroxetine Hydrochloride IPA solvate and Isotretinoin due to the benefit of smaller crystal size that it provided [15].

Many works in literature have shown the benefits of continuous crystallization in flow crystallizers namely rapid mixing time, constant conditions at steady state and narrow crystal size distribution. An example of achieving rapid mixing in continuous anti-solvent crystallization of Salicylic acid was shown by Brown *et al*. [7] in a Continuous Oscillatory Baffled Crystallizer (COBC). The crystallizer was ϕ15 mm x 700 mm in size. The technique they used was anti-solvent crystallization with 2-propanol as solvent and water as anti-solvent. They could achieve 884 g of product or 61 % yield in 6.25 hours of operation for solute concentration of 0.096 g/mL, solution flow rate of 40 mL/min and supersaturation of 5.56. A plug flow crystallizer was developed by Alvarez *et al*. [1] for pharmaceutical compounds. Anti-solvent crystallization of ketoconazole with methanol as solvent and water as anti-solvent was

investigated. The flow rates of the solution were in the range of 76 – 122 mL/min with channel diameter of 12.7 mm. They achieved smaller sizes in their plug flow reactor with a narrow size distribution. However, they found fluctuations in the growth rate of crystals due to the interaction of crystals with the mixer elements. A continuous crystallization setup for anti-solvent crystallization of pharmaceutical compounds was patented by Suslick *et al.* [16]. The design incorporated an ultrasonic horn in a T-mixer. The solution with the pharmaceutical compounds was supplied through an inlet within the horn. The main purpose of the design was to control particle sizes. There was no temperature control. The concern with using ultrasound horns is promotion of heterogeneous crystallization and contamination due to erosion [17].

Continuous flow sonocrystallization combines the benefit of reproducibility of crystal properties from the continuous part and benefits like intense mixing and cavitation from the ultrasound part. However, there is still a need to investigate the different crystallizer designs that will make sonocrystallization reach industry level scale up. In line with this idea, this work investigates anti-solvent sonocrystallization in a flow crystallizer. Acetyl Salicylic acid (ASA) is used as a model compound. Some works have already shown how ASA crystallization can be improved by ultrasound in batch. Miyasaka *et al*. [18] [19] investigated cooling sonocrystallization of ASA with Acetic acid as solvent. The experiments were carried out in a batch setup. An ultrasonic horn, working at 20 kHz and 50 W, was immersed in the solution. The solution was placed in a thermal bath for cooling. The solution was cooled from a maximum of 47 ^{0}C to 30 ^{0}C at a rate of 0.7 ^{0}C/min. The authors noticed that above a minimum power (4.5 W net ultrasonic power), ultrasound accelerated nucleation and the crystal sizes were much smaller due to the higher nucleation sites. Eder *et al*. [9] investigated continuous cooling crystallization of Acetyl-Salicylic acid (ASA) in a tubular crystallizer. In their setup an ultrasound bath was used to generate seeds of the compound from an ethanol solution of ASA. Two solution streams, one with seeds in the solution and the other without, were mixed in a Y-mixer. After the Y-mixer, a 27 m long channel was used to have four stages of cooling from 40 ^{0}C to 26 ^{0}C. The flow rates with a channel inner diameter of 2 mm were in the range of 5 – 15 mL/min. A separate inlet was used to pump in air to have a narrow residence time distribution. They found that ultrasound helped in achieving a narrow crystal size distribution. They could achieve higher yield and also reduce blocking which was predominant in their experiments without ultrasound. A couple of works have focused on experimenting and optimizing strategies for combined cooling and anti-solvent crystallization of ASA but without ultrasound in batch or MSMPR systems [20] [21] [22]. To the authors' best knowledge, the effect of anti-solvent sono-crystallization parameters like anti-solvent wt. %, initial concentration and power on the nucleation and yield of ASA in a tubular crystallizer has not been studied in literature.

This work focuses mainly on continuous, pure, seedless, anti-solvent crystallization of ASA in a tubular flow crystallizer with ultrasound. This work shows the potential of tubular crystallizers for continuous sonocrystallization of pharmaceutical compounds like ASA. Experiments are carried out in silent and sonicated conditions to clearly establish the effect of ultrasound. Nucleation of ASA crystals at different supersaturations is analyzed. Two ultrasonic powers are tested and yield is compared. Finally, particle size distribution is shown for some experiments to provide an idea of the achievable crystal sizes.

Materials and Methods

Materials

99% pure Acetyl Salicylic Acid (ASA) was purchased from Sigma-Aldrich. Absolute Ethanol (99% pure), purchased from Fisher –Scientific, was used as solvent. Distilled water was used as anti-solvent. All chemicals were used as obtained.

Experimental setup

A flow reactor developed by John *et al*. [23] for liquid-liquid extraction is used for anti-solvent sonocrystallization of ASA. The reactor is constructed as an aluminum housing with solid contact points at regular intervals that support PFA tubing. The housing provides space for cooling water circulation in order to control the temperature of the PFA channels. The assembly of the aluminum housing and PFA channels is bolted to an ultrasonic transducer. A transparent plexi-glass plate is used to cover the top part of the reactor. In this design, the transducer is not in direct contact with the process fluids, therefore, preventing contamination from erosion and eliminating additional external surfaces that can induce heterogeneous crystallization (nucleation occurring due to reduced interfacial free energy from the presence of external surfaces like ultrasonic horns). All experiments were carried out with the solution and anti-solvent pre-heated to 25 ^{0}C. The solubility of ASA in ethanol and water mixtures was obtained from literature [22]. Two pulse-free gear pumps (ISMATEC REGLO-Z digital, Z186 pump head) were used to pump the solution and anti-solvent. The pumps had a capacity range of 0.85 to 85 mL/min with steps of 0.02 mL/min. The solution and anti-solvent were heated to 25 ^{0}C with IKA® heating plates. The crystallizer had 50 cm (from 'Y' connector to point of exit) of Perfluoroalkoxy (PFA) tubing of inner diameter 2 mm and outer diameter 3 mm (Bola Germany). A Lauda© thermal bath (Silver ECO 620) with a Pt100 thermocouple was used to control the temperature of the crystallizer. The maximum pump speed providing a water circulation rate of 22,000 mL/min was selected. The crystallizer was bolted to an ultrasonic transducer (Ultrasonics World© MPI-7850D-20 40 60H). The frequency was maintained constant at 42 kHz. This was controlled with an *EI* 1020L radio frequency power amplifier and signal generator. A Pico© TC-08 thermocouple data logger with type-K thermocouples was used for temperature recording. Fig. 1 shows an illustration of the experimental setup.

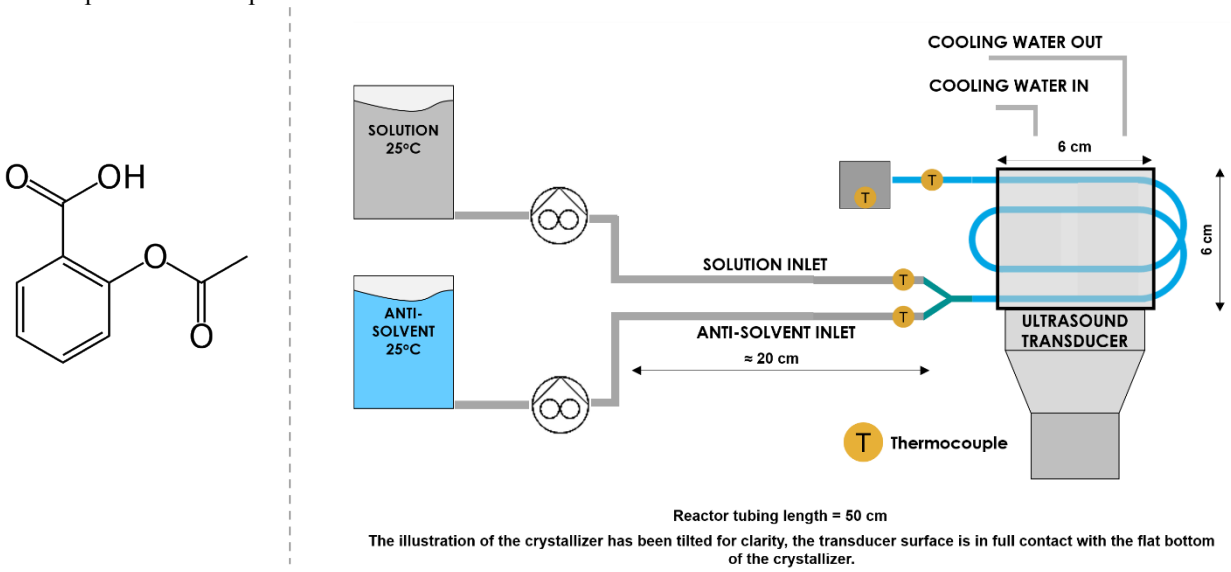

Fig. 1 (left) Molecular structure of Acetyl Salicylic Acid (Aspirin), (right) Illustration of the experimental setup.

Analysis of crystallization

For each initial concentration, a specific amount of ASA was weighed and added to a measured volume of ethanol. The mixture was stirred at 800 rpm for at least 2 hours while the temperature was controlled at 25 ^{0}C using the stirring plate. Distilled water was simultaneously temperature-controlled at 25 ^{0}C on a separate plate. The channels of solution and anti-solvent were combined by a 'Y' connector, with bore size of 1.5 mm, right before entering the crystallizer. Length of tubing between the 'Y' connector and the crystallizer was 1/10th (5 cm) of the total tubing length. Hence, a single stream of solution with anti-solvent entered the crystallizer. Experiments were first carried without ultrasound to establish the boundaries of supersaturation at which crystallization can occur within the crystallizer. In the next set of experiments, ultrasound was applied to see how that boundary is affected. The main variables in the experiments are the initial concentrations of ASA in ethanol and the wt. % (solute free basis) of water. Time for appearance of

crystals was recorded based on visual detection which is also shown as a reliable method for noticing crystallization [24]. Crystallization in the channels was highly recognizable due to the manifest change in transparency. An example of two cases, one without any crystallization and one with crystallization, is shown in Fig. 2. Temperature was recorded at the inlet streams of the solution and anti-solvent and at the outlet of the crystallizer. Supersaturation was varied in two ways – a) by varying the initial concentration of ASA in ethanol and b) by varying the wt. % of anti-solvent. Different anti-solvent wt. %s were obtained by varying the flow rate of the anti-solvent while keeping the solution flow rate constant. The solubility of ASA in pure ethanol at 25 ^{0}C is 237.9 g-ASA/kg-ethanol. Further in the manuscript g-ASA/kg-ethanol is represented as g/kg. The tested starting concentrations were 150 g/kg, 200 g/kg, 237.9 g/kg, 250 g/kg and 300 g/kg. Concentrations above saturation limit were tested to have conditions with high supersaturation. For the starting concentrations of saturation and above, i.e. 237.9 g/kg, 250 g/kg and 300 g/kg, 20 wt. % water was added to ethanol to completely dissolve ASA. The added water is taken in to consideration when determining the anti-solvent wt.%. This solution was filtered with a 2.7 μm filter. Experiments were conducted 3 times to ensure reproducibility. Supersaturation is calculated as a ratio of calculated concentration of ASA for certain wt. % and the 25 ^{0}C solubility concentration at that wt. %.

Experiments without ultrasound were conducted beginning with a low initial concentration of 150 g/kg. The flow rate of solution for these experiments was set to the lowest flow rate of 0.85 mL/min to provide maximum residence time in the crystallizer. The experiment was conducted for 15 min (which is at least 20 residence times). During this time observations for noticing crystallization were made in the channels and also in the beaker where the outflowing mixture of the solution and anti-solvent was collected. Experiments were conducted with the goal of identifying the lowest anti-solvent wt.% where crystallization without ultrasound would be possible. In next set of experiments ultrasound was used to enable crystallization in the channels and to investigate the boundaries of anti-solvent wt. % and supersaturation where crystallization can occur. To study the effect of steady state some experiments were conducted with a certain waiting time and the crystal detection time in such experiments was studied. All residence times mentioned are based on the combined flow rates of the solution and anti-solvent for each experiment.

In experiments with ultrasound it was noticed that heat generation due to enthalpy of ethanol- water mixing and cavitation led to re-dissolution within the channels [25]. Therefore a lower ultrasonic power was used to tackle this problem and yields at different powers were compared. Yield analysis was carried out for the experiment at 250 g/kg initial concentration, 70 wt.% anti-solvent and supersaturation of 3.07. In this experiment, the outflowing slurry was instantaneously filtered with a 0.22 μm filter in a vacuum filtration setup. The residue was allowed to air dry for at least 36 hours. To avoid losses and errors the filtered crystals were weighed with the filter and the dry weight of the filter was then subtracted. After this measurement, the yield was calculated based on the dissolved weight of ASA, as per Eq. 1.

$$Yield\ \% = \frac{Mass\ of\ crystals\ collected\ at\ outlet * 100}{Mass\ of\ crystals\ initially\ dissolved\ in\ that\ volume} \quad (1)$$

The calorimetric power was calculated by flowing only water through the crystallizer and with temperature control. Therefore net calorimetric power is presented here, based on mass flow rate of water, specific heat and change in temperature. (see Eq. 2). The tested powers are 24 ± 2 W at an amplitude was 550 mVolt which accounted to calorimetric power of 248 W/l and 7 ± 1 W at an amplitude – 300 mvolt which accounted to calorimetric power of 67 W/l)

$$Cal.\ power, W/l = \frac{\dot{m}_{water} *\ c_p * (T_{out} - T_{in})}{Reactor\ volume} \quad (2)$$

Particle size analysis

Particle size distributions were studied with the objective providing an idea of the achievable crystal sizes and for comparing particle sizes at different supersaturations. Samples used for this analysis were collected at the outlet after immediate vacuum filtration (0.22 μm filter) so as to avoid any growth after the crystallizer. Samples were air dried for at least 36 hours. Particle size measurements were performed in a Malvern Mastersizer 3000 Hydro SV laser diffractometer. The dispersant used was hexane. Before sample analysis the background (hexane – 99.9%) was

analyzed. ASA was then added to the dispersant until the desired obscuration was reached. Each sample was measured 5 times The average of these values is presented. Between each sample, at least 3 cleaning cycles were conducted.

Table – 1 Parameters for particle size measurement

Parameter	Value
Dispersant volume	7 mL
Dispersant	Hexane - 99.9%
Obscuration	>3%
Refractive index of ASA	1.56
Stirring speed	1800 RPM
Relative standard deviation Dx 10	5%
Relative standard deviation Dx 50	3%
Relative standard deviation Dx 90	3%

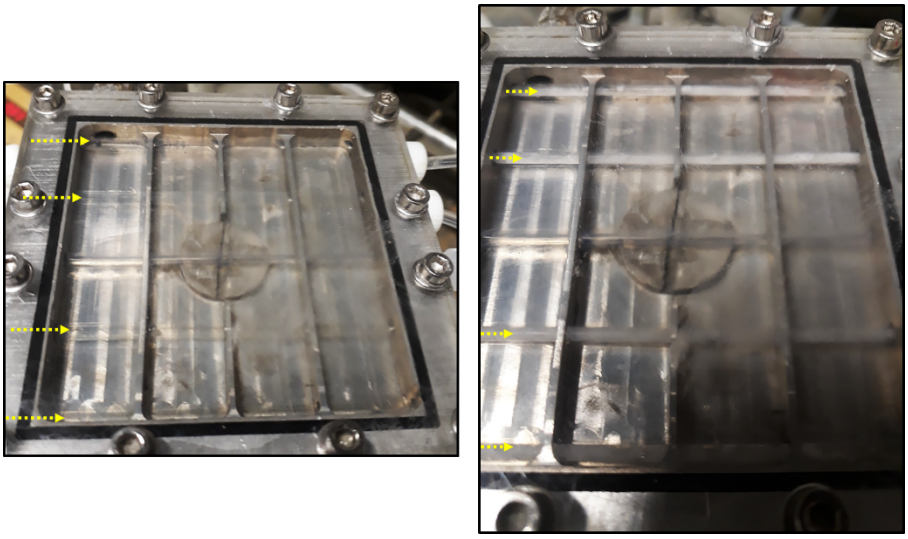

Fig. 2 Observation of crystals: (left) Experiment without ultrasound showing transparent channels (right) Experiment with ultrasound showing milky channels with crystals.

Results & Discussions

Experiments without ultrasound

Beginning with initial concentration of 150 g/kg, there was no nucleation in the crystallizer even at a supersaturation of 2.74 at anti-solvent wt. % of 78%, which is the maximum for this initial concentration.. However, there was crystallization detected immediately after exiting the crystallizer (in the collection beaker) even though there was no crystallization in the channels. Also, the temperature in the collection beaker was significantly higher (≈ 28 ^{0}C) than the temperature at the outlet (≈25.5 ^{0}C). The temperature rise in the beaker is seen in all cases irrespective of crystallization occurring. This is primarily due to the exothermic mixing of ethanol with water. If enthalpies of mixing at 25 ^{0}C are considered then the temperature rise can reach a maximum of 10 ^{0}C [25]. However, the temperature rise at the outlet when measured without the cooling bath was only about 2.5 ^{0}C indicating insufficient mixing. Further experiments were conducted at a higher initial concentration of 200 g/kg, 237.9 g/kg, 250 g/kg and 300 g/kg. Multiple supersaturation levels were tested by varying the anti-solvent wt. %, details are given in Table 2. The maximum supersaturation level possible in these conditions was 6.07 for 300 g/kg starting concentration and 80 wt. % of anti-

solvent. There was still no crystallization in the channels of the crystallizer which was also the case for other higher supersaturation levels tested: 4.91 at 250 g/kg – 80 wt. %, 4.64 at 237.9 g/kg – 79 wt. % and 3.61 at 200 g/kg – 76 wt. %. However, similar to experiments at 150 g/kg there was some crystallization after exiting the crystallizer. Therefore in experiments without ultrasound there was no crystallization in the crystallizer at any of the tested conditions, even at a high supersaturation of 6.07. Fig. 3 shows the phase diagram with details. Table. 1 provides the list of tested wt. %, flow rates and supersaturation levels.

This outcome gives two clear indications – a) that the induction time for these anti-solvent wt. % is larger than the experimental time scale at this level of mixing, b) mixing, which is crucial for anti-solvent crystallization [26], must be enhanced to induce nucleation within the crystallizer itself. These indications present a strong reason for testing ultrasound for this crystallizer, therefore at this stage experiments were conducted with ultrasound.

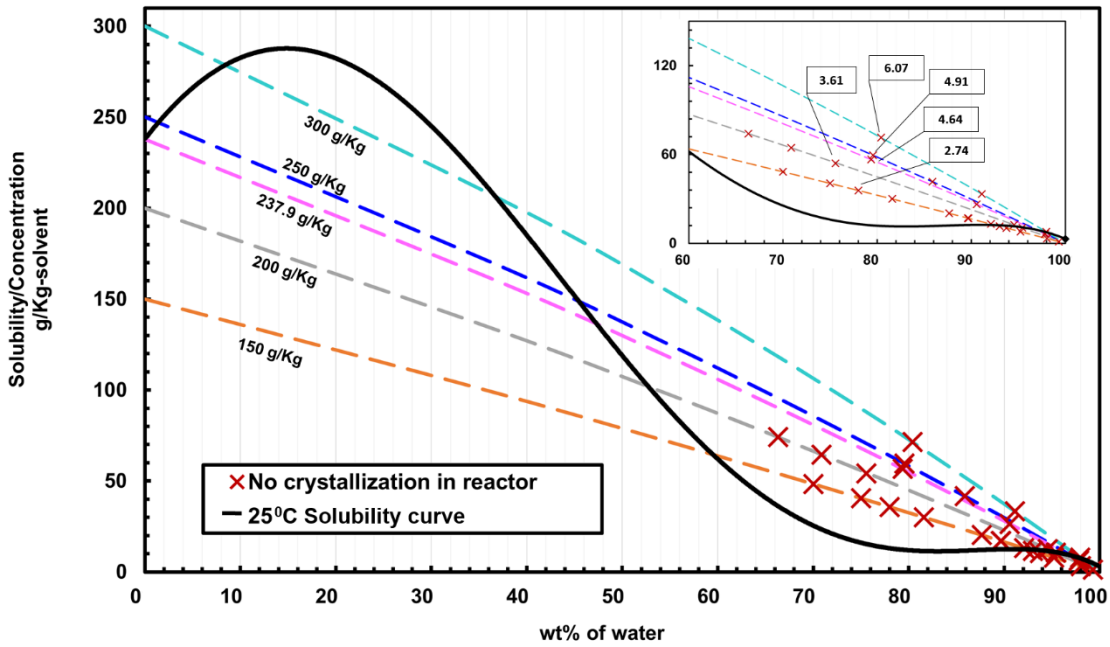

Fig. 3 Phase diagram of experiments without ultrasound. Solid black line represents the solubility curve at 25 ^{0}C for different anti-solvent wt.%. Dotted lines represent the working lines with possible concentrations that can be reached starting from each initial feed concentration. Red crosses represent the tested conditions. None of the tested conditions resulted in crystallization in the reactor. Supersaturation values are provided in boxes for points of highest supersaturation in each concentration line.

Table – 2 Details of flow rates and residence times for experiments without ultrasound.

Initial concentration	Solution Flow Rate - mL/min	Anti-solvent Flow Rate - mL/min	wt % of anti-solvent	Supersaturation	Residence time, s
150 g/kg	0.85	1.40	70	1.90	42
	0.85	1.80	75	2.52	35
	0.85	2.14	78	2.74	32
	0.85	2.67	82	2.57	27
	0.85	5.20	89.6	1.38	16
	0.85	5.24	90	1.32	15
	0.85	7.00	92	1.06	12
	0.85	8.00	93	1.00	11
	0.85	9.00	94	1.00	10
	0.85	12.0	95	1.00	7
	0.85	30.0	98	1.00	3
	0.85	85.0	99	1.00	1
200 g/kg	0.85	1.14	66	2.00	47
	0.85	1.41	71	2.78	42
	0.85	1.80	76	3.61	36
	0.85	10.0	95	1.02	9
	0.85	12.0	96	1.00	7
237.9 g/kg	0.85	2.14	79	4.64	32
	0.85	5.34	91	2.10	15
	0.85	25.0	98	1.00	4
250 g/kg	0.85	2.14	80	4.91	32
	0.85	3.34	86	3.55	23
	0.85	25.0	98	1.00	4
300 g/kg	0.85	2.14	80	6.07	32
	0.85	5.34	91	2.67	15
	0.85	25.0	98	1.02	4

Experiments with ultrasound - Effect of steady state:

Applying ultrasound enabled crystallization within the channels which was impossible in silent conditions. Further results are shown in the following paragraphs. However, it was observed that the time it takes for crystals to appear from the moment of application of ultrasound was much higher than the residence times and variable. The reason for this is speculated to be the lack of a steady state within the system which results in unstable distribution of the process fluids. In continuous flow crystallizers, achieving a steady state is important to have stable process conditions in the crystallizer [7]. For anti-solvent crystallization experiments this could influence the supersaturation homogeneity in the channel. Initially, the crystallizer channels are filled with air. When an experiment starts, the channels are completely primed with the process liquids, flowing with the corresponding flow rate of each experiment, in a duration of 1 residence time. At this point a steady state might not have been established. Therefore, further experiments were carried out to find the duration of steady state establishment and to establish the protocol for experiments with ultrasound. This tests also determined when ultrasound could be switched on during the experiments for better reproducibility. In these tests, the flow in one experiment was allowed to run for 1 residence time to prime the crystallizer before applying ultrasound and for 20 residence times more in a duplicate experiment. The time between completion of 1 residence time and application of ultrasound is further referred to as waiting time. Therefore, in the first experiment there was no waiting time while in the second experiment there was a waiting time of 20 residence times. The time between ultrasound application and the first noticeable crystals to appear (t_{cd} – s) is recorded. Experiments were also carried out at higher waiting times of 40 and 80 residence times. All experiments were at a

solution flow rate of 2 mL/min. Fig. 4 shows average t_{cd} of 3 identical experiments at different waiting times with error bars showing standard deviation within identical experiments. It is clearly seen that the deviation in cases where there is no waiting time is much higher than the cases in which there is some waiting time. The deviation already reduces from 45 s to 6.5 s for 20 residence time waiting and the difference in averages of 20, 40 and 80 residence time waiting are quite small compared to the difference with no waiting time and are within acceptable range compared to literature [5] [27] [28]. Further information is provided in the Appendix A. for steady state experiments at different solution flow rates.

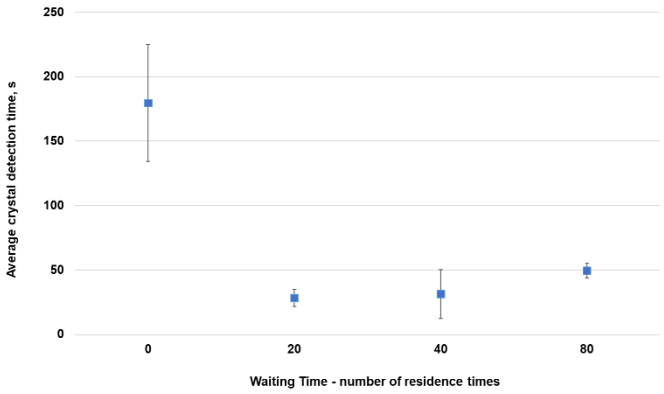

Fig. 4 Crystal detection time (t_{cd} - seconds) for steady state experiments: Experiments at constant solution flow rate of 2 mL/min (200 g/kg , 71%) and varying waiting times – 0, 20, 40 and 80 residence times. Squares represent average of 3 experiments and error bars show standard deviation within 3 identical experiments at each waiting time. See Fig. A.1 and A.2 in Appendix. A for t_{cd} in repeated experiments.

Crystallization with ultrasound – anti-solvent wt. % boundaries

Experiments were carried out to inspect the lowest anti-solvent wt. % limits at which crystallization can be achieved in the crystallizer at different initial concentrations. For each initial concentration, a high anti-solvent wt. % is tested first and then discrete experiments are conducted with reduced wt. % to the point where crystallization does not occur even with the assistance of ultrasound. The flow rates of solution (2 mL/min and 4 mL/min) were selected to provide a high residence time so that it is not a limitation for silent crystallization in the crystallizer. The comparison between crystallization in silent and sonicated conditions for each individual wt. % is performed at the same residence time. Flow rates for all experiments are given in Table 3.

For all experiments the net ultrasonic power applied was 24 ± 2 W . Without applying ultrasound there was no crystallization observed in the crystallizer for any of the tested conditions. Crystallization in the crystallizer channels was achieved only when ultrasound was used. Even for the lowest tested initial concentration of 150 g/kg, crystallization was successfully achieved with ultrasound. In this case, a high wt. % of 78 % (the point at which nucleation was observed in the collection beaker) was tested first showing successful crystallization in the crystallizer channels itself. Then experiments conducted at reduced wt. % and up to 72 wt. %, ultrasound could induce nucleation successfully. Below this, at 70 and 71 wt. %, there was no nucleation even with ultrasound. For the initial concentration of 200 g/kg ultrasound was applied from 71 wt. % and crystallization could still be achieved, apparently due to higher supersaturation. For this initial concentration crystallization could be achieved up to 64 wt. %. Below this point crystallization could not be achieved even with ultrasound.

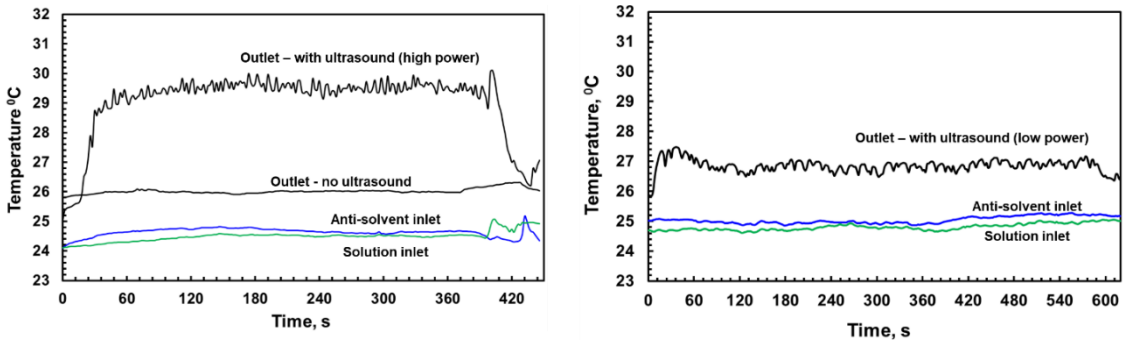

Fig. 5 Typical temperature plots: (left) During experiment at high-power ultrasound (24 W), (right) During experiment at low-power ultrasound (7 W).

Due to sonication there was a significant temperature rise in the channels irrespective of whether there is any crystallization or not and despite the cooling bath. The typical temperatures at outlet is shown in Fig. 5 (left). The outlet temperature recorded is close to 30 ^{0}C. The temperature rise within the channels is seen to have a noticeable effect for higher starting concentrations. For experiments at 237.9 g/kg, (saturation limit) crystallization could occur at as low as 49 wt. %, but these crystals would visibly re-dissolve in the channels at approximately half of total length, making the mixture flowing inside the channels transparent. This means that the supersaturation was sufficient to induce crystallization at 25 ^{0}C when the fluid mixture enters the crystallizer, but due to the temperature rise in the channels the crystals re-dissolve. A gradual reduction of re-dissolution compared to even low anti-solvent wt.% is seen from 57. wt.%. Small amount of crystals discontinuously make through the outlet but the re-dissolution effect is still evident. At least 61 wt. % was needed to get continuous crystallization (crystallization in the channels without re-dissolution). Similarly, for starting concentrations of 250 g/kg, crystallization could be achieved at 46 wt. % with re-dissolution, but at least 60 wt. % was needed for stable, continuous crystallization. For 300 g/kg at 38 wt. %, crystallization with re-dissolution was observed and at least 59 wt. % was needed for stable, continuous crystallization. The range of wt. % at which re-dissolutions are observed is as large as 21 % at 300 g/kg, which reduces to 14 % for 250 g/kg and further down to 12 % for 237 g/kg. This is explained by the large differences in solubility of ASA in ethanol-water mixtures at higher concentrations for different temperatures. The solubility gap narrows down with reduction in concentration, therefore the re-dissolution gap also reduces. Crystallization time in the experiments at 200 g/kg and 150 g/kg was mostly close to the residence times. While for higher initial concentrations the induction time for crystallization, whether continuous or re-dissolving ,was always in range of the residence time or shorter.

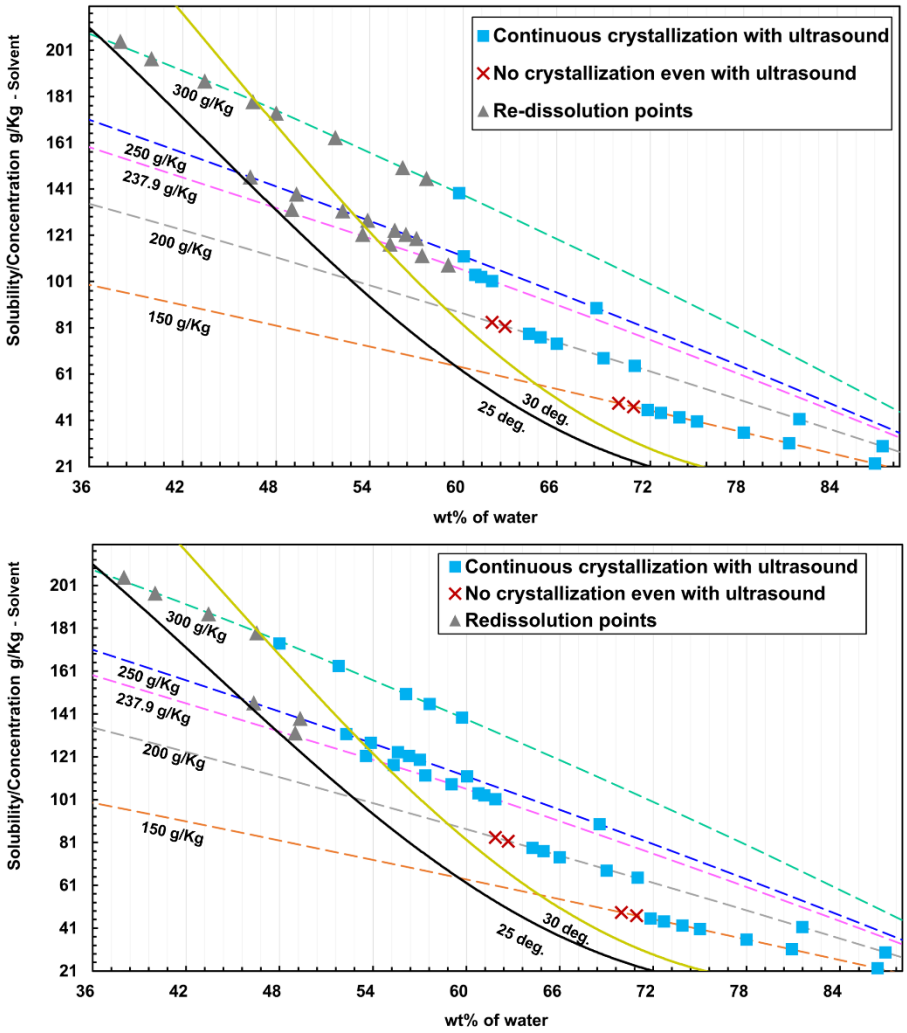

Fig. 6 Phase diagrams for experiments with ultrasound (top) for experiments at high ultrasound power (24 W) and (bottom) for experiments with low ultrasound power (7 W). Solid black line represents the solubility curve at 25 ^{0}C for different anti-solvent wt.%. Solid yellow line is the solubility curve for 30 ^{0}C. Dotted lines represent the working lines with possible concentrations that can be reached starting from each initial feed concentration. Blue squares are those conditions at which continuous crystallization was achieved. Red crosses are conditions at which there was no crystallization and grey triangles are conditions that showed re-dissolution.

Crystallization with low-power ultrasound and yield assessment

Cavitation is one of the causes for temperature rise in the channels along with heat of mixing and heat losses from ultrasound to the liquid (e.g. acoustic streaming etc.). To reduce temperature rise in the channels, ultrasound with lower net power was applied. The main idea was to reduce re-dissolutions in the channels and to investigate whether the wt. % limit for crystallization can be lowered for 200 and 150 g/kg initial concentrations. An ultrasound net power of 7 W ± 1 W was tested, to have the outlet temperature as close as possible to the outlet temperature in silent condition. In all tested cases there was a temperature reduction at the outlet of close to 3 ^{0}C compared to high-power experiments. Temperature plots are shown in Fig. 5 (right). Using low-power ultrasound was effective in aiding continuous crystallization at lower anti-solvent wt. % than before. Around 6 -10% reduction in the anti-solvent wt. % threshold for continuous crystallization is observed for starting concentrations of 237.9 g/kg to 300 g/kg. The least anti-solvent wt. % for continuous crystallization is 48 % at 300 g/kg initial concentration. For lower initial concentrations (200 g/kg and 150 g/kg), there was no change in the crystallization limits. This is reasonable

considering the low concentration and narrow difference in solubility at different temperatures in these conditions. Cavitation at high power was still insufficient to induce nucleation at these points, therefore, at low power also the result was poor. Fig. 6 presents the phase diagram for high-power experiments and the phase diagram with combined low-power experiments. An interpolated solubility curve for 30 ^{0}C is also added for better analysis. Some tests with even lower ultrasound power of 3 W were tried for wt. % at which re-dissolutions were still occurring but there was no crystallization. The hypothesis for this is the lack of sufficient cavitation due to low acoustic pressure, therefore further experiments at this low power level were not conductedThe applied calorimetric powers are comparable with the work of Miyasaka *et al.* [19] where batch, cooling, sono-crystallization of ASA was carried out at calorimetric powers in the range 35 to 110 W/L.

Low powers did reduce the occurrence of re-dissolution, but they possibly can also affect the yield. To check this, yield at both powers was analyzed at 250 g/kg initial concentration and 70 wt. %. Experiments were conducted at both powers (24 W and 7 W) and repeated 3 times. In each experiment the product was collected for 3 minutes ± 5 sec. since the onset of crystallization. Fig. 7 presents the yields. Results showed that the yield for experiments at lower power was slightly higher than the yield for high power. The average yield for experiments at high power was 31.6 %, whereas for low power it was 35.2 %. A student t-test (one tail, paired) results in probability of 0.058 which makes the difference not statistically significant. At lower supersaturation levels the yield difference is significant since low power ultrasound provides some yield which was otherwise zero due to re-dissolution. Considering there was at least no reduction in the yield, the application of low ultrasonic power is recommended for such flow crystallizers in order to utilize the benefit of ultrasound, but at the same time avoid as much as possible thermal changes. In terms of the MSZW, ultrasound is seen to induce nucleation for really narrow supersaturation levels of 1.02, 1.02 and 1.05 for 300, 250, and 237.9 g/kg, respectively. This width broadens for 200 and 150 g/kg where nucleation is induced at supersaturation of 1.76 and 2.16. Fig. 8 provides a better visualization of the MSZW with respect to supersaturation. The supersaturation curves for various starting concentration lines are plotted along with the experimental data points.

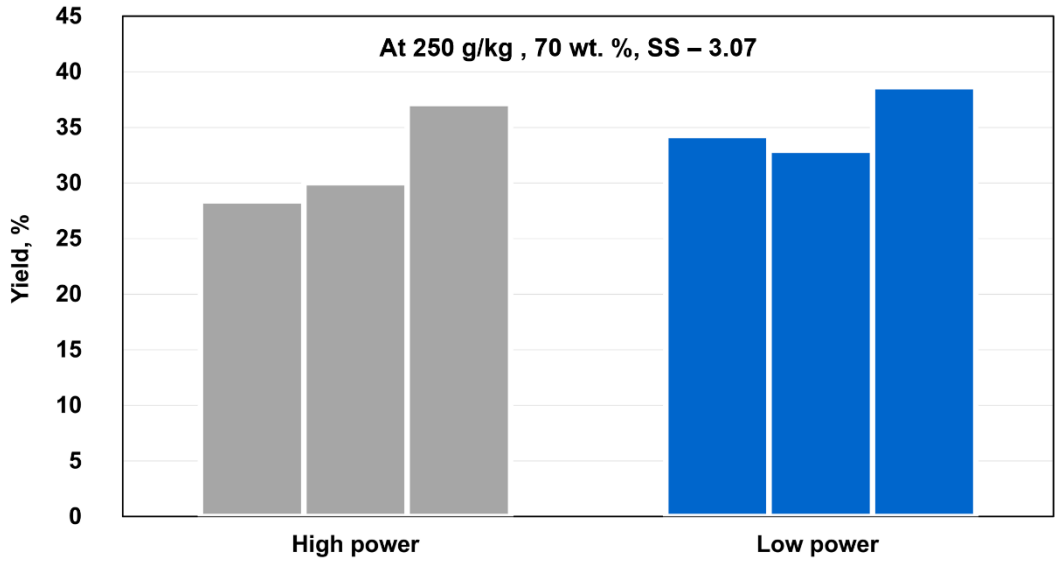

Fig. 7 Yield for experiments comparing different powers. High power – 24 ± 2 W, Low power – 7 ± 1 W.

Table 3 Details of flow rates and residence times for experiments with ultrasound. (Bold- continuous crystallization, shaded – re-dissolution, un-bolded – no crystallization)

Initial Concentration	Sol. Flow Rate - mL/min	Anti-sol.Flow Rate - mL/min	Anti-sol. wt. % High power	Anti-sol. wt. % Low power	Super saturation	Residence time, s	Crystal detection time, s
150 g/kg	2	3.30	70	70	1.90	18	-
	2	3.47	71	71	2.03	17	-
	2	3.61	**72**	**72**	2.16	17	112
	2	3.77	**73**	**73**	2.30	16	58
	2	4.00	**74**		2.41	15	25
	2	4.25	**75**		2.52	15	28
	2	5.02	**78**		2.74	13	23
	2	6.00	**81**		2.67	12	5
	2	9.00	**87**		1.88	9	6
200 g/kg	2	2.20	62	62	1.55	22	-
	2	2.28	63	63	1.63	22	-
	2	2.43	**64**	**64**	1.76	21	103
	2	2.51	**65**	**65**	1.88	21	92
	2	2.63	**66**		1.99	20	95
	2	3.00	**69**		2.44	19	34
	2	3.32	**71**		2.78	18	28
	2	6.00	**82**		3.60	12	10
	2	9.00	**87**		2.50	9	6
237.9 g/kg	4	2.51	49	49	1.05	14	18
	4	3.01	54	**54**	1.25	13	26
	4	3.23	55	**55**	1.35	13	12
	4	3.52	57	**57**	1.49	13	29
	4	3.77	59	**59**	1.62	12	12
	4	4.05	**61**	**61**	1.78	12	5
	4	4.11	**61**	**61**	1.82	12	6
	4	4.24	**62**		1.90	11	6
250 g/kg	4	2.23	46	46	1.02	15	23
	4	2.51	49	49	1.13	14	14
	4	2.83	52	**52**	1.26	14	10
	4	3.01	54	**54**	1.34	13	14
	4	3.23	56	**56**	1.45	13	12
	4	3.33	56	**56**	1.49	13	11
	4	3.42	57	**57**	1.55	13	8
	4	3.88	**60**		1.80	12	10
	4	5.63	**70**	**70**	3.07	10	5
300 g/kg	4	1.50	38	38	1.02	17	19
	4	1.63	40	40	1.07	17	15
	4	1.88	43	43	1.16	16	14

	4	2.13	47	47	1.26	15	15
	4	2.26	48	**48**	1.32	15	14
	4	2.63	52	**52**	1.52	14	13
	4	3.13	56	**56**	1.83	13	10
	4	3.33	58	**58**	1.96	13	6
	4	3.63	**60**		2.19	12	5

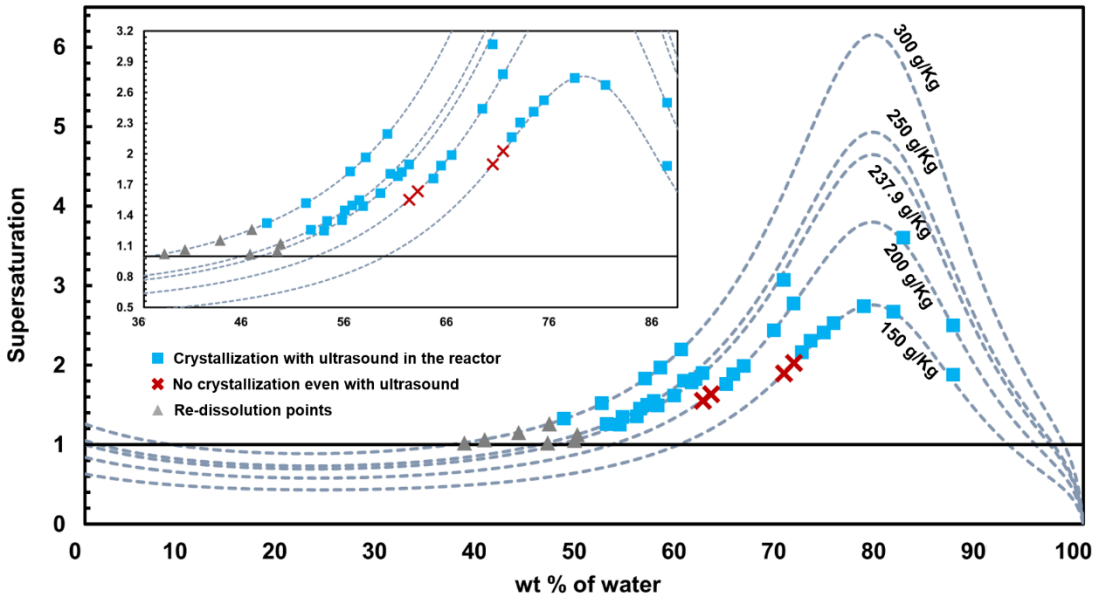

Fig. 8 Supersaturation plots (dotted lines) for different starting concentrations and all experimentally tested data points – (Supersaturation is calculated with respect to solubility at 25 ^{0}C. Experiments at low power 7±1 W).

Static experiments

To study the reason why there was no crystallization in the channels without ultrasound some experiments were conducted to compare the differences in induction time. In these experiments the point where the supersaturation is highest (6.07 at 300 g/kg, 80 wt. % – See Table -1) is chosen. The solution flow rate is set to the lowest flow rate of 0.85 mL/min, the corresponding anti-solvent flow rate is 2.14 mL/min and the residence time is 32 seconds. The flow is allowed to run for 20 residence times and then stopped and the mixture in the channels is allowed to stay static. Therefore the mixture inside the channels is given the time needed to nucleate. By keeping the mixture static in the channels, a very high residence time is provided for nucleation as in batch, but at the interaction levels of a flow system. Ultrasound was not applied at any time and the reactor was constantly monitored visually and with a microscope. Crystals were seen in the system only after at least 6 hours. However in another experiment the same procedure was repeated but ultrasound (24 ± 2 W) was switched on when the flow was stopped. There was spontaneous crystallization visible in the system (within 5-7 seconds). These experiments were repeated 3 times and the same results were observed (see Fig. 9). This gives us the information that the induction times of the system are much higher than the residence times. The reason for this is the enhanced mixing and presence of cavitation resulting from ultrasound, therefore leading to effective crystallization in the channels. Such reduction in induction time for anti-solvent crystallization has been shown in literature for organic compounds like Roxythromycin [8] and in-organic compounds like Sodium chloride [12].

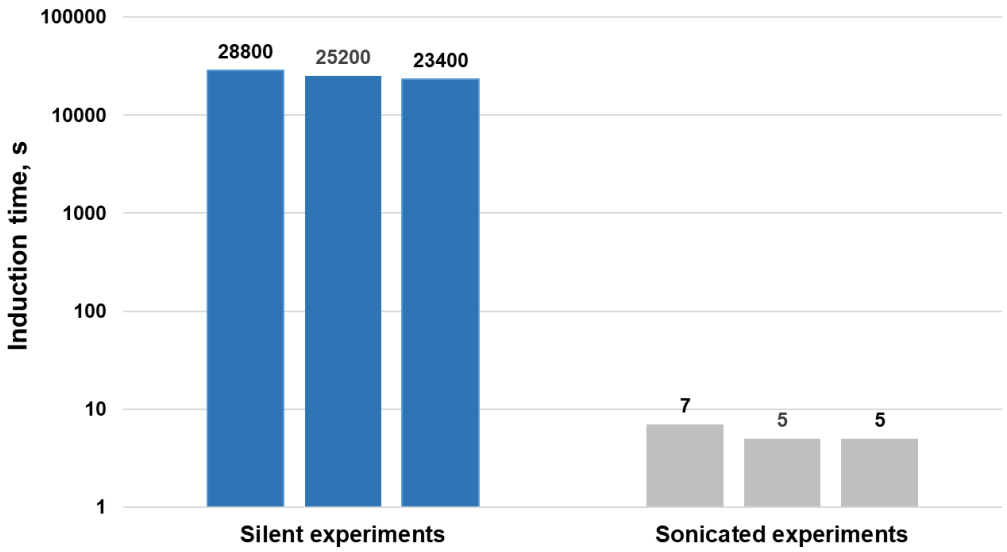

Fig. 9 Induction time (crystal detection time) for experiments conducted in static conditions with and without ultrasound.

Particle size distribution (PSD)

PSD analysis is carried out in this study to get an estimate of crystal sizes that can be produced through sonocrystallization experiments in this type of crystallizer. Six samples collected from different experiments are analyzed. Three samples are collected from experiments with initial concentration of 200 g/kg and three from 150 g/kg. Table 4 gives the details of the flow rates, wt. % and supersaturation levels. Multiple works [29] [30] have shown a decrease in particle size with ultrasound. Fig. 9 shows the particle size distribution based on volume density. For 150 g/kg experiments, the particle size of obtained crystals in the average range of 4.3 µm (Dx 10) to 46 µm (Dx 90). For 200 g/kg the average particle sizes are in the range of 4 µm (Dx 10) to 26 µm (Dx 90). Varying the supersaturation level by anti-solvent wt.% does not seem to have a significant effect on particle sizes since there is negligible difference in the sizes of crystals for experiments of same initial concentration but different anti-solvent wt.%. One would expect that, at higher supersaturation levels, crystal sizes would be smaller but that doesn't seem to be the case [31]. It must be mentioned here that particle sizes can also be influenced by cavitation bubble sizes and numbers [29] which could be a reason for the absence of a specific trend in particle sizes. In addition to that, temperature changes within the crystallizer can also affect the supersaturation. However, mean crystal sizes for higher starting concentration of 200 g/kg seem to be slightly smaller than that for 150 g/kg which could be due to high supersaturation in 200 g/kg compared to 150 g/kg.

Table – 4 Details of flow rates, residence times and sizes for PSD experiments.

Initial concentration	Solution Flow Rate - mL/min	Anti-solvent Flow Rate - mL/min	Anti-solvent wt %	Supersat.	Residence time, s	Dx10 mm	Dx50 mm	Dx90 mm
150 g/kg	2	4	74%	2.39	16	4.33	17.0	45.5
	2	6	81%	2.67	12	5.85	19.7	44.2
	2	9	86%	1.89	9	5.93	17.8	36.7
200 g/kg	2	3	69%	2.42	20	3.98	11.2	30.8
	2	6	82%	3.61	12	3.85	11.0	21.8
	2	9	87%	2.49	9	3.97	12.3	26.2

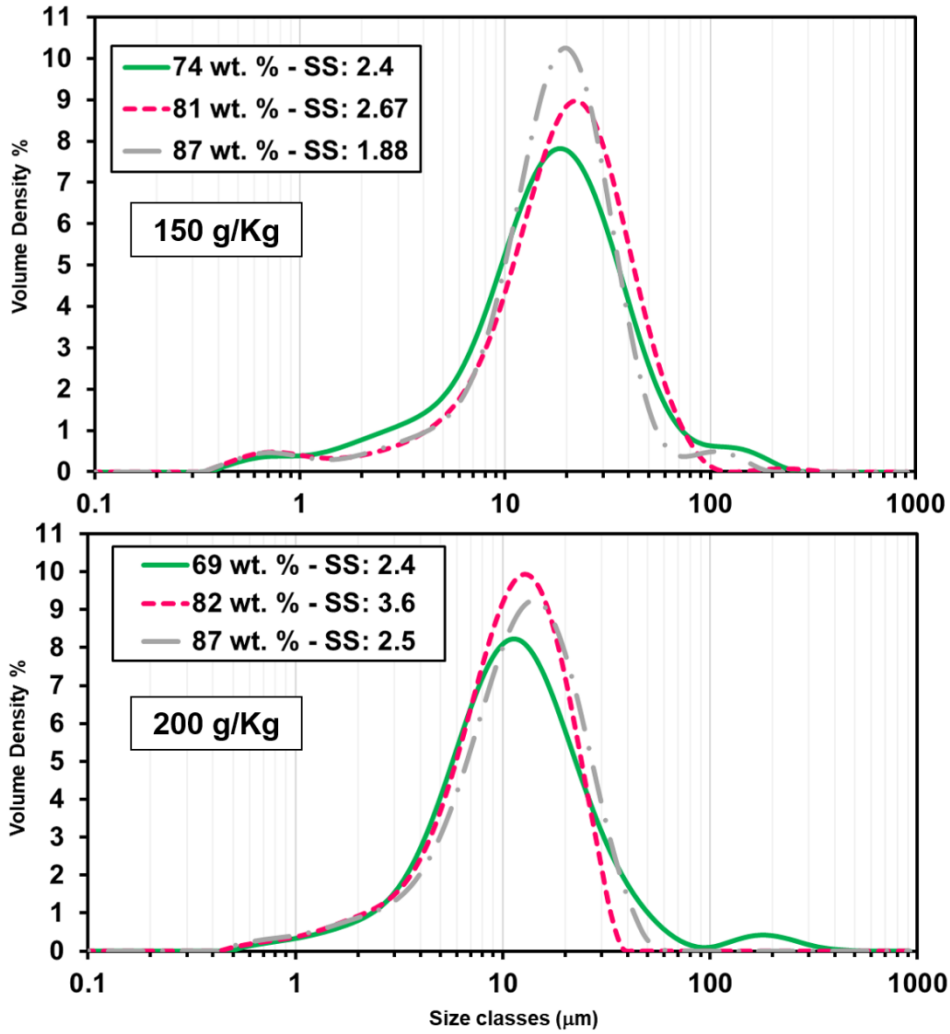

Fig. 9 Particle size distributions (top) for different conditions at 150 g/kg and (bottom) for different conditions at 200 g/kg.

Conclusions

Anti-solvent sonocrystallization in a flow crystallizer was studied in this work. Acetyl Salicylic acid (ASA-Aspirin) was used as a model compound. Experiments were carried out in silent and sonicated conditions to investigate the parameters at which crystallization could be achieved in the flow crystallizer. Five different initial concentrations were tested. At each initial concentration the anti-solvent wt. % was varied. In silent experiments, there was no crystallization in any of the tested conditions. The use of ultrasound made it possible to achieve effective crystallization within the crystallizer. Lack of steady state in the crystallizer caused higher and irreproducible crystallization times. Experiments with multiple waiting times showed that a waiting time of 20 residence times before applying ultrasound is sufficient to have a steady state in the crystallizer which leads to lower and reproducible crystal detection times.

Ultrasound application in this flow crystallizer setup is accompanied with temperature rise despite applying a cooling bath. This led to a re-dissolution of crystals within the channels for experiments with initial concentration of saturation limit and above. The wt. % up to which re-dissolutions occurred was 59 % for 300 g/kg, 60 % for 250 g/kg and 61 % for 237.9 g.kg. To overcome this, low-power ultrasound was tested which reduced the temperature rise in the channels. The yield of experiments at high and low power were compared. Low-power ultrasound was effective in enabling continuous crystallization to a large extent without any losses in the yield, in fact, with slightly higher yield. Continuous crystallization was now achieved at 48 wt.%, 52 wt. % and 54 wt. % for 300 g/kg, 250 g/kg and 237.9 g/kg, respectively. There was no loss in yield for crystallization at low-power.

Particle sizes were analyzed for some experiments and the particles were in the size range of 4 µm to 46 µm. Supersaturation variation with different anti-solvent wt. % does not seem to have an effect on the particle sizes. But supersaturation variation with initial concentration does seem to provide smaller crystal sizes.

In conclusion, this work demonstrates that continuous anti-solvent crystallization for pharmaceuticals like ASA can be achieved with ultrasound in flow crystallizers. Ultrasound significantly accelerated nucleation in the channels of the crystallizer and enabled crystallization even at low supersaturation levels. With use of ultrasound continuous crystallization was achieved for an anti-solvent wt. % as low as 48% (supersaturation of 1.02). It was found that using lower power ultrasound was more effective in achieving continuous crystallization without loss in yield. The work also demonstrates the potential of this particular type of tubular crystallizer design for anti-solvent crystallization of pharmaceutical compounds. Further optimization can be achieved by modifying the crystallizer design to have smaller channel lengths, lower residence times or different cooling liquids to any thermal changes.

Acknowledgements

The research leading to these results has received funding from the European Community's Horizon 2020 Programme [(H2020/2016 – 2020) under Grant Agreement no. 721290 (MSCA-ETN COSMIC)]. This publication reflects only the author's view, exempting the Community from any liability. Project website: https://cosmic-etn.eu.

References

[1] A. J. Alvarez and A. S. Myerson, "Continuous Plug Flow Crystallization of Pharmaceutical Compounds," *Crystal Growth & Design*, vol. 10, no. 5, pp. 2219-2228, 2010.

[2] A. Vancleef, S. Seurs, J. Jordens, T. Van Gerven, L. C. J. Thomassen and L. Braeken, "Reducing the Induction Time Using Ultrasound and High-Shear Mixing in a Continuous Crystallization Process," *Crystals*, vol. 8, no. 326, 2018.

[3] J. Chen, B. Sarma, J. M. B. Evans and A. S. Myerson, "Pharmaceutical Crystallization," *Crystal Growth and Design*, vol. 11, pp. 887-895, 2011.

[4] J. Ulrich and P. Frohberg, "Problems, potentials and future of industrial crystallization," *Front. Chem. Sci. Eng.*, vol. 7, no. 1, pp. 1-8, 2013.

[5] G. M. Maggioni and M. Mazzotti, "Modelling the stochastic behaviour of primary nucleation," *Faraday Discussions*, vol. 179, 2015.

[6] D. Zhang, S. Xu, S. Du, J. Wang and J. Gong, "Progress of Pharmaceutical Continuous Crystallization," *Engineering*, vol. 3, pp. 354-364, 2017.

[7] C. J. Brown, J. A. Adelakun and X.-w. Ni, "Characterization and modelling of antisolvent crystallization of salicylic acid in a continuous oscillatory baffled crystallizer," *Chemical Engineering and Processing: Process Intensification*, vol. 97, pp. 180-186, 2015.

[8] Z. Guo, M. Zhang, H. L. J. Wang and E. Kougoulos, "Effect of ultrasound on anti-solvent crystallization process," *Journal of Crystal Growth*, vol. 273, pp. 555-563, 2005.

[9] P. E. Rafael J, S. Schrank, M. O. Besenhard, E. Roblegg, G.-W. Heidrun and J. G. Khinast, "Continuous Sonocrystallization of Acetylsalicylic Acid (ASA): Control of Crystal Size," *Crystal Growth and Design*, vol. 12, p. 4733−4738, 2012.

[10] B. Gielen, J. Jordens, J. Janssen, H. Pfeiffer, M. Wevers, L. C. J. Thomassen, L. Braeken and T. Van Gerven, "Characterization of stable and transient cavitation bubbles in a milliflow reactor using a multibubble sonoluminescence quenching technique," *Ultrasonics Sonochemistry*, vol. 25, pp. 31-39, 2015.

[11] L. H. Stanley, "The effect of ultrasonic vibrations on crystallization processes," *Ultrasonics*, 1967.

[12] J. Lee and S. Yang, "Antisolvent Sonocrystallisation of Sodium Chloride and the Evaluation of the Ultrasound Energy Using Modified Classical Nucleation Theory," *Crystals*, vol. 8, no. 320, 2018.

[13] J. Lee, K. Yasui, M. Ashokkumar and S. E. Kentish, "Quantification of Cavitation Activity by Sonoluminescence To Study the Sonocrystallization Process under Different Ultrasound Parameters," *Crystal Growth and Design*, vol. 18, pp. 5108-5115, 2018.

[14] M. D. L. d. Castro and F. Priego-Capote, "Ultrasound-assisted crystallization (sonocrystallization)," *Ultrasonics Sonochemistry*, vol. 14, pp. 717-724, 2007.

[15] G. Ruecroft, D. Hipkiss, T. Ly, N. Maxted and P. W. Cains, "Sonocrystallization: The Use of Ultrasound for Improved Industrial Crystallization," *Organic Process Research & Development*, vol. 9, pp. 923-932, 2005.

[16] K. S. Suslick, B. W. Zeiger and H. N. Kim, "Ultrasonic method and apparatus for producing particles having a controlled size distribution". Patent US20160008782A1, 2018.

[17] S. Mottyll and R. Skoda, "Numerical 3D flow simulation of ultrasonic horns with attached cavitation structures and assessment of flow aggressiveness and cavitation erosion sensitive wall zones," *Ultrasonics Sonochemistry*, vol. 31, pp. 570-589, 2016.

[18] E. Miyasaka, Y. Kato, M. Hagisawa and I. Hirasawa, "Effect of ultrasonic irradiation on the number of acetylsalicylic acid crystals produced under the supersaturated condition and the ability of controlling the final crystal size via primary nucleation," *Journal of Crystal Growth*, vol. 289, pp. 324-330, 2006.

[19] E. Miyasaka, S. Ebihara and I. Hirasawa, "Investigation of primary nucleation phenomena of acetylsalicylic acid crystals induced by ultrasonic irradiation—ultrasonic energy needed to activate primary nucleation," *Journal of Crystal Growth*, vol. 295, pp. 97-101, 2006.

[20] Y. Yang and Z. K. Nagy, "Model-Based Systematic Design and Analysis Approach for Unseeded Combined Cooling and Antisolvent Crystallization (CCAC) Systems," *Crystal Growth & Design*, vol. 14, pp. 687-698, 2013.

[21] Y. Yang and Z. K. Nagy, "Combined Cooling and Antisolvent Crystallization in Continuous Mixed Suspension, Mixed Product Removal Cascade Crystallizers: Steady-State and Startup Optimization," *Ind. Eng. Chem. Res*, vol. 54, pp. 5673-5682, 2015.

[22] C. Lindenberg, M. Krattli, J. Cornel and M. Mazzotti, "Design and Optimization of a Combined Cooling/Antisolvent Crystallization Process," *Crystal Growth & Design*, vol. 9, no. 2, pp. 1124-1136, 2009.

[23] J. J. John, S. Kuhn, L. Braeken and T. Van Gerven, "Ultrasound assisted liquid–liquid extraction with a novel interval-contact reactor," *Chemical Engineering and Processing: Process Intensification*, vol. 113, pp. 35-41, 2017.

[24] M. Fujiwara, P. S. Chow, D. L. Ma and R. D. Braatz, "Paracetamol Crystallization Using Laser Backscattering and ATR-FTIR Spectroscopy: Metastability, Agglomeration, and Control," *Cryst. Growth Des.*, vol. 2, pp. 363-370, 2002.

[25] J. A. Boyne and A. G. Williamson, "Enthalpies of mixture of ethanol and water at 25.degree.C," *J. Chem. Eng. Data,*, vol. 12, no. 3, p. 318, 1967.

[26] Y. Dong, W. K. Ng, J. Hu, S. Shen and R. B. H. Tan, "A continuous and highly effective static mixing process for antisolvent precipitation of nanoparticles of poorly water-soluble drugs," *International Journal of Pharmaceutics*, vol. 386, pp. 256-261, 2010.

[27] D. Kashchiev, D. Verdoes and G. M. v. Rosmalen, "Induction time and metastability limit in new phase formation," *Journal of Crystal Growth*, vol. 110, no. 3, pp. 373-380, 1991.

[28] C. Lindenberg and M. Mazzotti, "Effect of temperature on the nucleation kinetics of α l-glutamic acid," *J. Cryst. Growth*, vol. 311, pp. 1178-1184, 2009.

[29] H. N. Kim and K. S. Suslick, "The Effects of Ultrasound on Crystals: Sonocrystallization and Sonofragmentation," *Crystals*, vol. 8, no. 280, 2018.

[30] J. Jordens, E. Canini, B. Gielen, T. Van Gerven and L. Braeken, "Ultrasound Assisted Particle Size Control by Continuous Seed Generation and Batch Growt," *Crystals*, vol. 7, no. 195, 2017.

[31] K. Wohlgemuth, F. Ruether and G. Schembecker, "Sonocrystallization and crystallization with gassing of adipic acid," *Chemical Engineering Science*, vol. 65, pp. 1016-1027, 2010.

Appendix. A

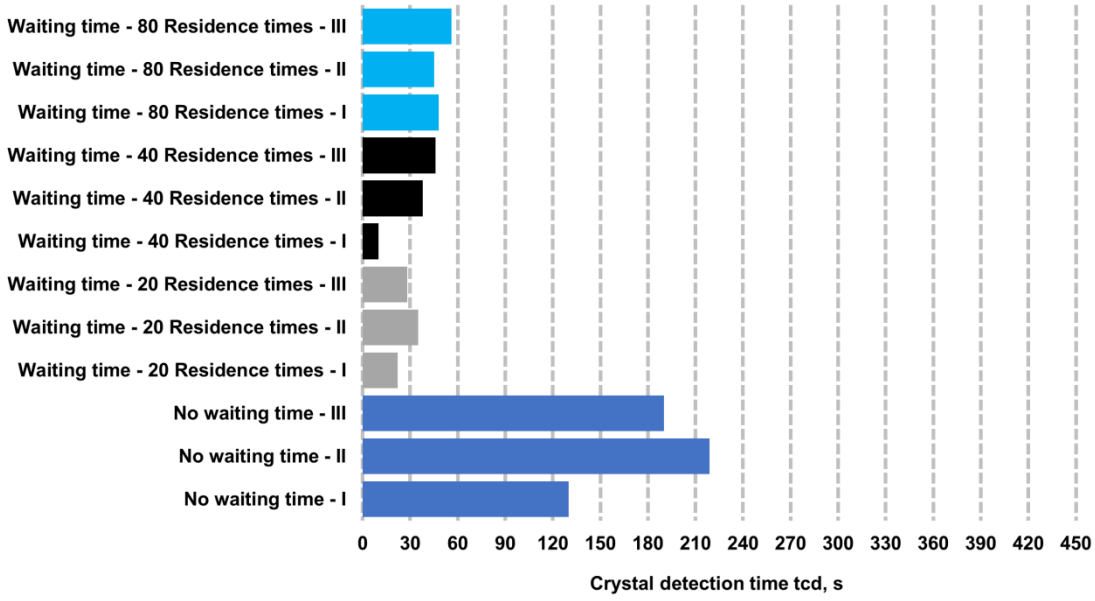

Fig. A.1 Crystal detection times for each waiting time case.

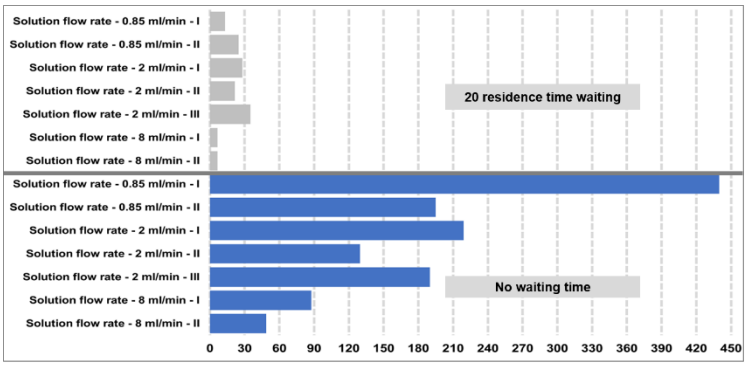

Fig. A.2 Crystal detection times for experiments are different flow rates.

Steady state experiments were also carried out for different flow rates and the same effect is seen. This is done for 3 sets of experiments having the same initial concentration and anti-solvent wt.% (200 g/kg-ethanol, 71wt. %), but with different flow rates. The solution flow rates for these experimental sets were 0.85 mL/min, 2 mL/min and 8 mL/min. The anti-solvent flow rates corresponding to these experiments were 1.4 mL/min, 3.3 mL/min and 13.2 mL/min respectively. The residence times in these experiments were 42 s, 18 s and 4.2 s respectively. Fig. A.2 shows the crystal detection time for different flow rates and different waiting times. It was noticed that when there was no waiting time t_{cd} was much higher than the residence time and there was a large difference in observed t_{cd} for the replicate experiments. For solution flow rate of 0.85 mL/min, t_{cd} varies between 3 min to 7 mins which is close to 10 residence times. For solution flow rate of 2 mL/min, t_{cd} was always above 2 minutes (7 residence times) and highest was above 3 minutes (12 residence times). For the highest solution flow rate of 8 mL/min, t_{cd} fluctuated between 1 minute (15 residence times) and 1.5 minutes (21 residence times). The maximum t_{cd} in these experiments was 21 residence times, which was the basis for selecting a waiting time of 20 residence times instead of a lower value. When a waiting of 20 residence times is applied, t_{cd} is much smaller than the earlier observed times of 7 min or 3 min in the experiments with no waiting time. For 0.85 mL/min and 2 mL/min, this reduced to less than 30 seconds and for 8 mL/min this reduced to merely 7 seconds.

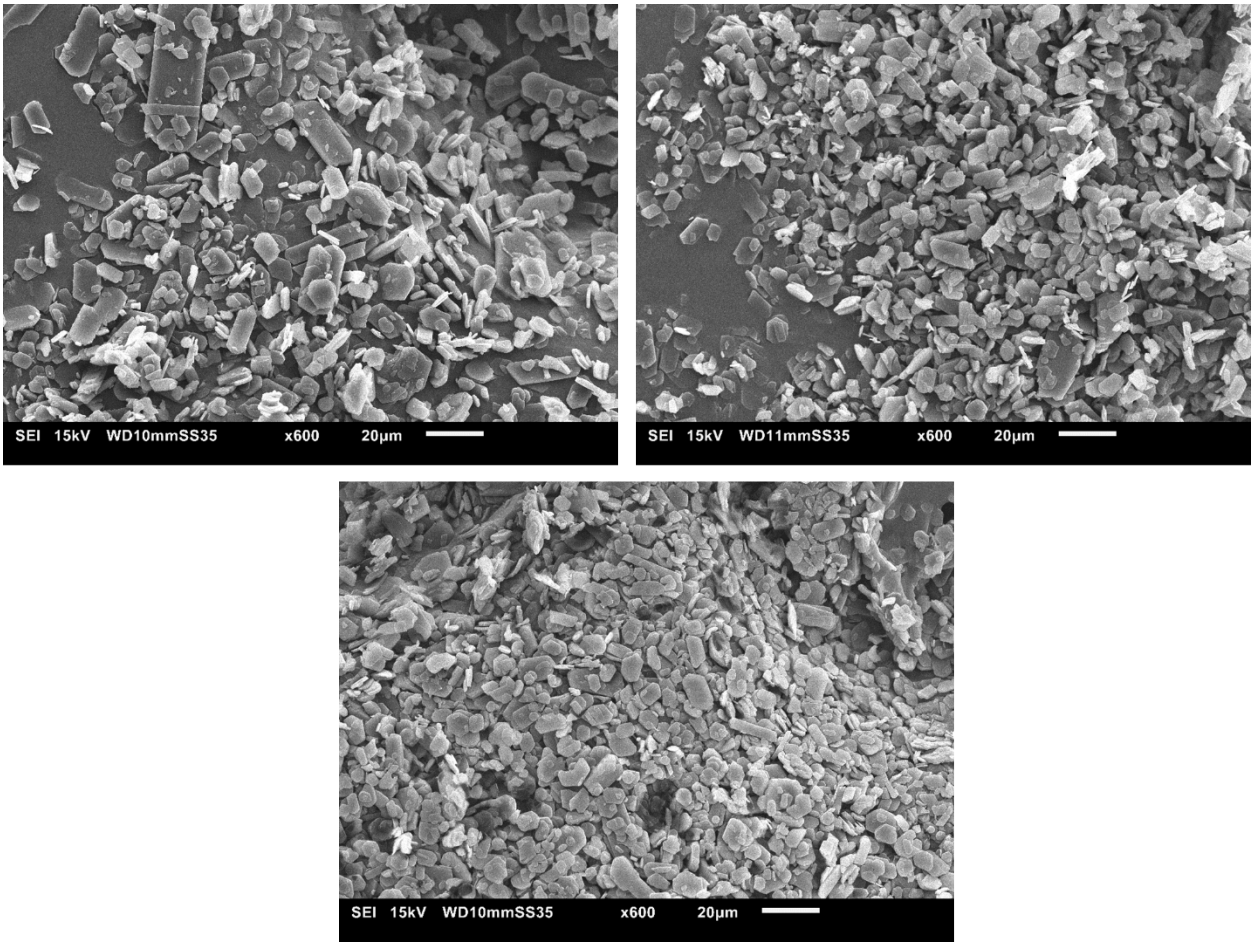

Fig. A.3 Scanning Electron Microscope images of ASA (Aspirin) produced in crystallization experiments with ultrasound. All images are for experiments with initial concentration of 200 g/kg at a power of 24 ± 2 W, the anti-solvent wt. % and supersaturation are (from top left) 69% and 2.4, 82% and 3.6, 87% and 2.5.

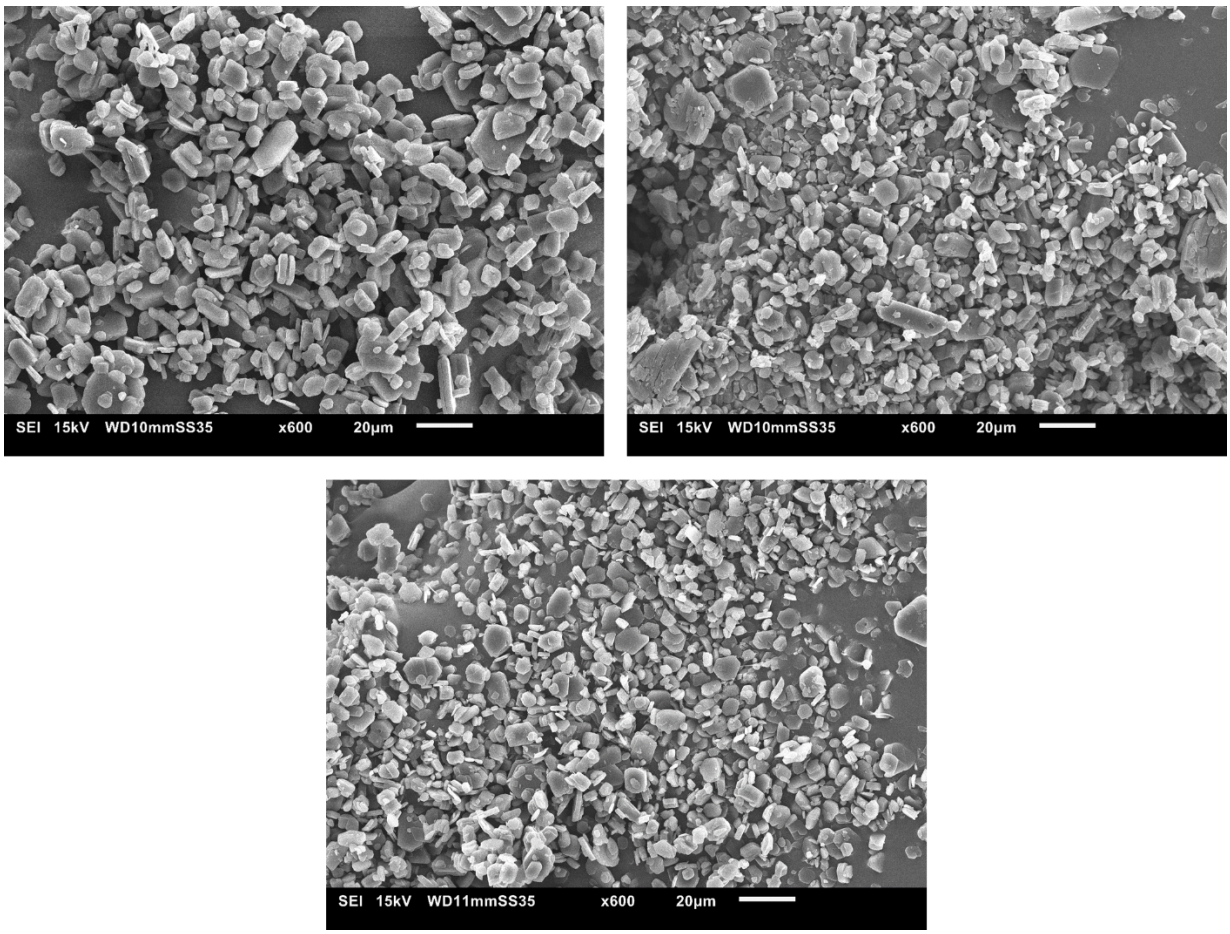

Fig. A.4. Scanning Electron Microscope images of ASA (Aspirin) produced in crystallization experiments with ultrasound. All images are for experiments with initial concentration of 150 g/kg at a power of 24 ± 2 W, the anti-solvent wt. % and supersaturation are (from top left) 74% and 2.4, 81% and 2.67, 87% and 1.88.